COGNITIVE NEUROSCIENCE

Cognitive chimera states in human brain networks

Kanika Bansal[1,2,3]*, Javier O. Garcia[1,4], Steven H. Tompson[1,4], Timothy Verstynen[5], Jean M. Vettel[1,4,6], Sarah F. Muldoon[3,7]*

The human brain is a complex dynamical system, and how cognition emerges from spatiotemporal patterns of regional brain activity remains an open question. As different regions dynamically interact to perform cognitive tasks, variable patterns of partial synchrony can be observed, forming chimera states. We propose that the spatial patterning of these states plays a fundamental role in the cognitive organization of the brain and present a cognitively informed, chimera-based framework to explore how large-scale brain architecture affects brain dynamics and function. Using personalized brain network models, we systematically study how regional brain stimulation produces different patterns of synchronization across predefined cognitive systems. We analyze these emergent patterns within our framework to understand the impact of subject-specific and region-specific structural variability on brain dynamics. Our results suggest a classification of cognitive systems into four groups with differing levels of subject and regional variability that reflect their different functional roles.

INTRODUCTION

Rhythmic behavior is ubiquitous in complex systems, and a diverse set of research has examined how interacting system elements come together to form synchronized, coherent behavior across domains that span biological, social, and engineered settings (*1*). However, the emergence of complete system-wide synchronization might not always provide the best description of system dynamics. In many systems, states of partial synchrony have been observed, where a system organizes in separate domains of synchronized elements (*2*, *3*). This is particularly true in the human brain, where patterns of neurophysiological activity evolve rapidly, showing transient domains of synchronization across subsets of brain regions (*2*). In the past decade, the rise of network neuroscience approaches (*4*) have demonstrated a foundational role for partial synchrony among separate cognitive subnetworks, where the underlying architecture of the brain ensures efficient integration of sensory input with stored knowledge while also segregating task-irrelevant information to support cognition (*5*). However, the fundamental principles and constraints that subserve the intricate timing and specificity of these time-evolving patterns of synchrony are not well understood (*6*).

The dynamical systems framework of chimera states offers a powerful tool to study the evolution of coherent and incoherent dynamics in oscillating systems such as the brain. A chimera state emerges when a system of oscillators evolves into two subsets of mutually coherent and incoherent populations (*7*). Although chimera states represent a natural link between coherent and incoherent dynamics (*8*), initially, they were found and explored only analytically in the networks of homogeneous phase oscillators (*9*, *10*), and their relationship to real physical systems was unknown. It was not until almost a decade after their theoretical discovery that chimera states were demonstrated experimentally (*11*, *12*), lastly establishing their connection with real-world systems. Subsequently, chimera states were studied in a variety of model systems under different coupling schemes, including global (*13*) and purely local (*14*) connections, and their presence in oscillating systems was found to be more abundant than previously thought (*15*) [for an overview of studies on chimera states, see the recent review by Panaggio and Abrams (*7*)]. Chimera states have also been found to emerge under the presence of noise (*16*) and in heterogeneous networks (*17*). Given these findings, in the past few years, new classifications of chimera states, such as multichimera (*18*), traveling chimera (*19*), and chimera death (*20*), have been defined on the basis of the specific spatiotemporal dynamics involved.

Because of its natural ability to describe patterns of partial synchronization, the chimera framework has an intuitive utility for augmenting our understanding of the brain. Patterns of synchronization between cognitive systems are thought to form the basis of cognition, and the interplay of synchrony among subsets of brain regions has been shown to be important both in normal brain function, for example, in the variability in task performance (*5*), and in the continuum between healthy and disease states (*21*). Recent work has speculated that similarities exist between chimera states and brain dynamics during unihemispheric sleep (*7*) and the transition to a seizure state in epilepsy (*22*). Fundamentally, these dynamics are the result of complex interactions between neuronal populations and are often modeled using networks of coupled oscillators. As a result, despite the intuitive similarities between chimera states and brain dynamics, much of the work relating chimera dynamics to neuroscience, thus far, has focused on understanding chimera states at the level of neuronal networks, using mathematical modeling of networks of individual neurons with fewer elements and/or simplified connection topologies (*18*, *23*). Only recently have neuronal models been used to examine the possibility of the emergence of chimera-like states within large-scale brain networks derived from two well-characterized animal brains—*Caenorhabditis elegans* (*24*) and the cat cortex (*25*). However, even in these instances, the network connectivities were modified for simplicity. Thus, there remains a gap between studies of chimera states and applications to large-scale functional patterns of brain activity thought to underlie cognition. This largely reflects the computational complexity of modeling whole-brain dynamics and identifying an informative, yet simplified, model of cognitive processing.

Here, we bridge this gap by presenting a cognitively informed, chimera-based framework combined with in silico experiments (*26*), where we leverage the existence of a core set of predefined cognitive

[1]Human Research and Engineering Directorate, U.S. Army Research Laboratory, Aberdeen Proving Ground, MD 21005, USA. [2]Department of Biomedical Engineering, Columbia University, New York, NY 10027, USA. [3]Mathematics Department, University at Buffalo, SUNY, Buffalo, NY 14260, USA. [4]Department of Biomedical Engineering, University of Pennsylvania, Philadelphia, PA 19104, USA. [5]Department of Psychology, Carnegie Mellon University, Pittsburgh, PA 15213, USA. [6]Department of Psychological and Brain Sciences, University of California, Santa Barbara, Santa Barbara, CA 93106, USA. [7]CDSE Program and Neuroscience Program, University at Buffalo, SUNY, Buffalo, NY 14260, USA.
*Corresponding author. Email: phy.kanika@gmail.com (K.B.); smuldoon@buffalo.edu (S.F.M.)

systems that constitute the functional organization of the brain (*27*, *28*). Consequently, our framework keeps the computational complexity of the analysis to a minimum while providing the unique ability to connect chimera states as an underlying basis for cognition. Using personalized brain network models (BNMs), we study cognitive system–level patterns of synchrony that emerge across 76 brain regions within nine cognitive systems as the result of regional brain stimulation. Our analysis focuses on how brain architecture relates to the frequency and types of dynamical patterns produced after stimulation. More specifically, we aim to answer two questions: (i) Do patterns of synchronization observed for each cognitive system depend on what region was stimulated (region-specific effects) and (ii) does structural variability between participants decrease the consistency of patterns observed for each cognitive system (subject-specific effects)?

From our in silico experiments, we observe different patterns of synchronization that can be classified into three dynamical states: (i) a coherent state of global synchrony, (ii) a chimera state with coexisting domains of synchrony and desynchrony, and (iii) a metastable state with an absence of any large-scale stable synchrony. Our results demonstrate rich diversity in the states produced across all nine cognitive systems, including variability in patterns based on both region-specific and subject-specific structural variability. Critically, all nine cognitive systems give rise to chimera states, and this likely reflects the foundational role that partial synchrony serves in large-scale brain function. Neuronal dynamics must concurrently segregate specialized processing while integrating localized functions for coordinated, cohesive cognitive performance. Our chimera-based framework provides an avenue to study how dynamical states give rise to variability in cognitive performance, providing the first approach that can uncover the link between chimera states and cognitive system functions that subserve human behavior.

RESULTS

We first build subject-specific BNMs using anatomical connectivity derived from diffusion spectrum imaging (DSI) data of 30 healthy individuals. We have previously shown that these data-driven BNMs, combined with in silico experiments, can successfully explain individual variability in performance across certain language-based cognitive tasks (*26*). In the present work, we leverage these computational BNMs to understand the structural constraints to the macroscopic cognitive organization of the brain. The steps to construct a BNM are illustrated in Fig. 1A. We first parcellate the brain into 76 regions (network nodes) and define weighted network edges based on structural connectivity between brain regions. The dynamics of each brain region are modeled using Wilson-Cowan oscillators (WCOs), a biologically inspired, nonlinear mean-field model of a small population of neurons (*29*). The coupling between regions is derived on the basis of the unique structural connectivity of each individual (fig. S1). When multiple WCOs are coupled, the resulting patterns of synchronization are highly dependent on the topology of the coupling, ensuring that these BNMs are highly sensitive to individual variability in the underlying anatomical connectivity (*27*, *30*). As illustrated in Fig. 1B and fig. S1, we then perform in silico experiments by systematically applying computational regional (nodal) stimulation to the BNM. Previous work using in silico brain stimulation has studied the impact of local perturbations on large-scale brain dynamics (*31*) and shown that stimulation of certain regions can produce activity patterns that are similar to resting-state activity of the brain (*32*). Here, we focus on assessing the resulting patterns of synchronization that emerge on the basis of subject-specific and region-specific variation in structural connectivity as a result of computational regional stimulation.

Classification of brain states using cognitive systems

Traditionally, one would measure system-wide synchronization by calculating a measure such as the Kuramoto order parameter within the entire network of oscillators (*33*). However, we are interested in exploring how the stimulation of different brain regions drives brain function and how brain function is constrained by variability in structural connectivity. Therefore, we instead focus on the relationship between patterns of synchronization among experimentally motivated cognitive systems, where the regions assigned to each system have been shown to support similar cognitive processes. Thus, on the basis of previous research (*27*, *28*), we assigned each of the 76 brain regions into one of nine cognitive systems (fig. S2). Each cognitive system is defined by regions that coactivate in support of a generalized class of cognitive functions. This delineation includes several sensory motor–related systems, including auditory (Aud), visual (V), and motor and somatosensory (MS) systems, as well as the ventral temporal association system (VT) that encapsulates regions involved in knowledge representation. Several of the systems are involved in functional roles that are generic across cognitive performance, including the attention system (Att), the medial default mode system (mDm), and two systems associated with cognitive control, the cingulo-opercular (CP) and frontoparietal (FP) systems. Last, we include the subcortical system that consists of the regions responsible for autonomic and primal functions.

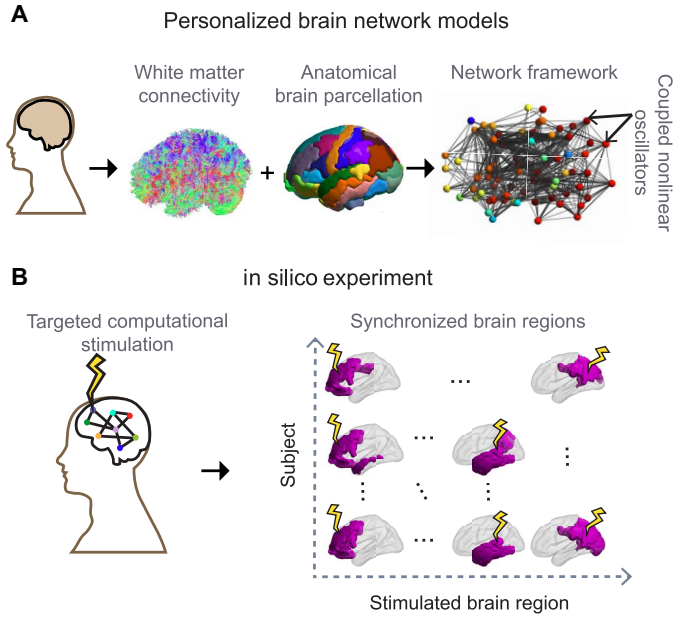

Fig. 1. Design of the in silico experiments. (**A**) We construct personalized BNMs by estimating white matter anatomical connectivity of the brain using DSI. This connectivity is combined with a brain parcellation scheme with 76 cortical and subcortical regions to obtain a large-scale connectivity map of the regional brain volume. These regions constitute the nodes of the structural brain network whose dynamics are simulated by nonlinear WCOs, coupled through the structural connectivity map of a given subject (see Materials and Methods). (**B**) In the resulting data-driven models of the spatiotemporal dynamics of the brain, each brain region is systematically stimulated across a cohort of 30 subjects. The spread of the stimulation is measured through synchronization within the brain network.

In each in silico experiment, we stimulate a brain region in each subject-specific BNM and then compute the cognitive system–level synchronization. Specifically, we calculate a cognitive system–based Kuramoto order parameter $\rho_{si,sj}$ that measures the amount of synchrony among all oscillators (regions) within two cognitive systems s_i and s_j and obtain a cognitive system–based synchronization matrix, as shown in Fig. 2A. In this synchronization matrix, we define two cognitive systems, s_i and s_j, to be synchronized if $\rho_{si,sj}$ exceeds a threshold value ρ_{Th}. In Fig. 2A, we chose $\rho_{Th} = 0.8$ to define three dynamical states observed in this study: (i) a coherent state, where all cognitive systems are synchronized; (ii) a cognitive chimera state, where some cognitive systems form a synchronized cluster (yellow) while the other systems remain incoherent (blue); and (iii) a metastable state, where no stable synchrony between cognitive systems is observed. In a metastable state, we observed oscillator populations to exhibit transient states of synchrony and desynchrony [metastability (*34*)] and the absence of a long-range stable synchronization. This state is characterized by a high metastability index (Materials and Methods) and is distinct from coherent and chimera states (fig. S3).

Next, we compare our cognitive system–based analysis with two traditional measures of synchronization: (i) the classical Kuramoto order parameter (*33*) calculated across all 76 oscillators (regions) that captures the level of global synchrony in the network and (ii) the chimera index (*24*, *34*) that describes the closeness of the state with an ideal chimera state (see Materials and Methods). In Fig. 2B, we show how the three dynamical states (coherent, chimera, and metastable) observed after stimulation of different brain regions in different subjects are distributed in the global synchrony and chimera-index parameter space. Each dot in this figure denotes a single brain region that was stimulated, its position denotes the amount of global synchrony and chimera index it produced in the network, and its color represents the classification of the emergent state within our cognitive framework. In the parameter space of the global synchrony and chimera index, we observe a separation in the area occupied by these states. As expected, global synchrony decreases from the coherent to chimera to metastable state. Thus, a cognitively informed, system-based classification of dynamical states is comparable to the traditional measures of estimating synchrony within a network.

We also examine how these two traditional metrics of synchronization relate to the connectivity properties of the node (region) itself. As seen in Fig. 2C, the level of global synchrony is positively correlated with the degree of the region being stimulated ($r = 0.81$; $P < 10^{-308}$). Stimulation of a network hub (highly connected brain region) is therefore more likely to produce a coherent state, while stimulation of a nonhub is more likely to result in either a chimera or metastable state. Figure 2D reveals that the chimera index shows a relatively weaker and negative correlation with the degree of the region stimulated ($r = -0.61$; $P = 6.4 \times 10^{-229}$). This relationship indicates the ability of moderately connected brain regions to produce a variety of spatially distinct synchronization patterns as a result of stimulation. These results not only demonstrate that chimera states emerge among large-scale cognitive systems, but also reveal that the variable structural connectivity of regions within cognitive systems can drive the whole brain into diverse synchronization patterns. It has been previously shown that the effectiveness of a brain region as a stimulation site is related to its position within the cortical hierarchy (*31*), and we therefore also examined whether the emergence of a cognitive state can be predicted by the connectivity between the stimulated region and the highly connected core, or rich club, of the brain (*35*). We obtained a set of core regions within each subject and then calculated the average shortest path length of each brain region to this core (see Materials and Methods). This quantity signifies the ease with which one can reach at a core region from a given region within the network. In Fig. 2E, we observe that the average shortest path length to the core correlates negatively with the global synchrony ($r = -0.74$; $P < 10^{-308}$). This indicates that, apart from the core itself, the regions that are easily connected to the core are also likely to produce a state with high synchrony. Here, colors identify the cognitive classification of the emergent states into coherent (red), chimera (yellow), and metastable (blue) states. Although we do not observe a direct separation of states based on the average shortest path length to the core, one can conclude that regions closest to the core are more likely to produce a coherent state, while regions farthest from the core are likely to produce a metastable state.

Variable brain states emerge from stimulation of different brain regions

Given that the type of brain state that emerges as result of stimulation is related to the network connectivity of the region, we next asked whether there is also a relationship between the location of the stimulated region and the type of dynamical state produced. In Fig. 3, brain regions are depicted as an orb, and their sizes denote the normalized occurrence of a given state that they produce upon stimulation, calculated across individuals. Regions that produce coherent states (network hubs) are distributed more closely to the midline of the brain (Fig. 3A, large nodes), while regions that produce the opposite extreme, metastable states, are distributed further from the midline, along the edges of the hemispheres (Fig. 3C, large nodes). Regions that produce chimera states are relatively uniformly distributed within the brain space (Fig. 3B). In fig. S4, we further quantify the relationship between the spatial location of a region, the degree of the region, and the dominant cognitive state produced when the region is stimulated. We did not observe a one-to-one mapping between these features but did observe qualitative trends, indicating that regions closer to the midline have higher degrees and are more likely to produce a coherent state than regions further from the midline with lower degrees that are more likely to produce a metastable state. These trends highlight differences in the structural organization of the brain that potentially aid in the fulfillment of different cognitive goals. Regions along the midline of the brain that produce a coherent state (e.g., subcortical regions such as the hippocampus and thalamus) can play a global cognitive role and facilitate communication between spatially separated brain regions. Conversely, regions located further from the midline produce metastable states, consistent with the notion that local and/or specialized computations take place in the cortex.

Because of the diversity in the distribution of dynamical states across spatially distributed regions, in Fig. 4, we investigate the relative contribution of the nine cognitive systems in producing each dynamical state after regional stimulation. Different systems contribute differently to observed dynamical states (coherent, chimera, and metastable), which provides a link between the observed states and their cognitive relevance. As shown in Fig. 4A, coherent states are produced predominantly by regional stimulation within subcortical and medial default mode systems, reflecting that many of their constituent regions are network hubs.

There is also system specificity for metastable states, which are preferentially produced by four systems (Fig. 4C). Two of those systems, the cingulo-opercular and frontoparietal, are associated

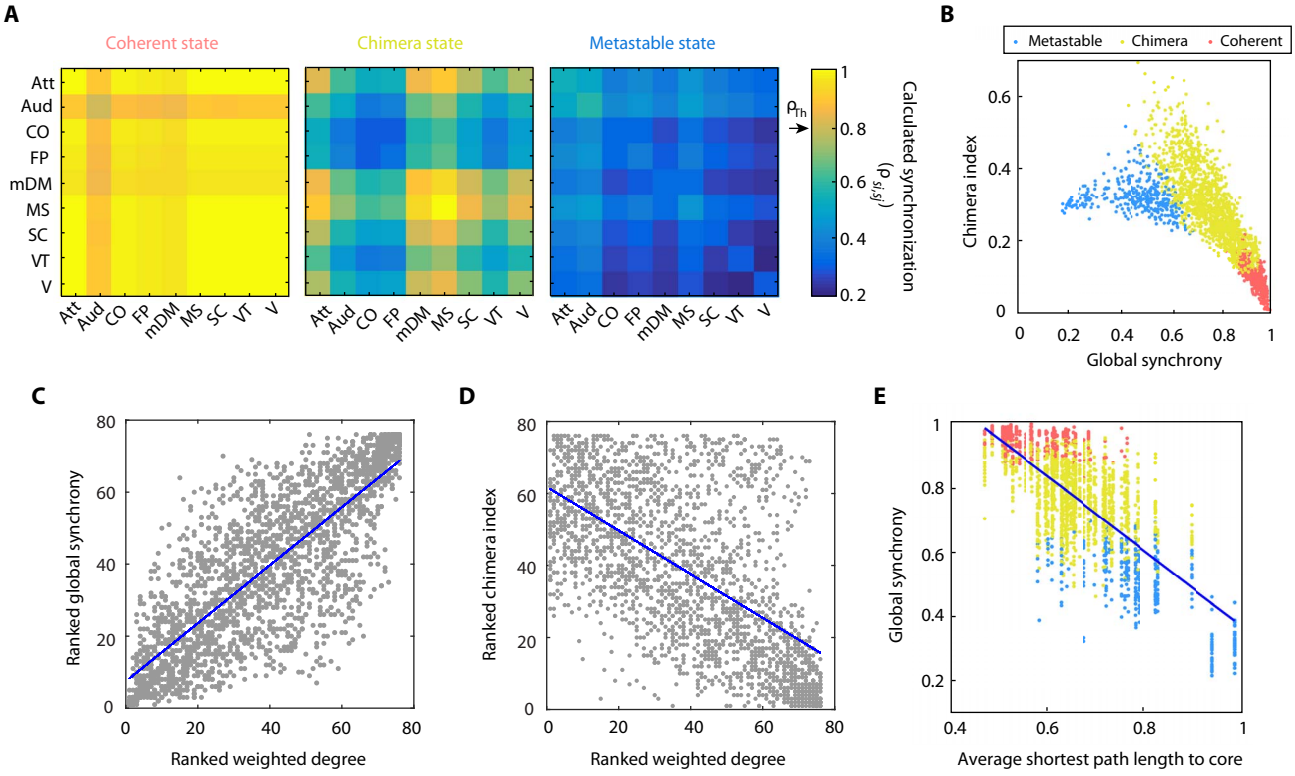

Fig. 2. Emergence of dynamical states within a cognitively informed framework. (**A**) Cognitive system–level synchronization matrices (whose entries denote the extent of synchronization between cognitive systems) for coherent, chimera, and metastable states. (**B**) Comparison of different frameworks. A dot represents a brain region in a subject, and its position indicates the global synchrony and chimera index (traditional measures) produced in the BNM upon stimulation of this region. The color of a dot identifies the classification of the emergent state into one of the cognitively defined states. A coherent state has a high global synchrony value and low chimera index (red). Both chimera (yellow) and metastable (blue) states show lower global synchrony. Since chimera states can comprise different patterns, they can have either a higher global synchrony or a higher chimera index than metastable states. (**C** to **E**) The origin of these states follows the connectivity of the stimulated brain region. (C) The global synchrony is positively correlated with the weighted degree of brain regions ($r = 0.81$; $P < 10^{-308}$), indicating that the network hubs are more likely to produce a coherent state. (D) The chimera index is weakly and negatively correlated with the weighted degree ($r = -0.61$; $P = 6.4 \times 10^{-229}$), indicating that stimulation of lower degree nodes is more likely to produce an ideal chimera state with half of the population synchronized and the other half desynchronized. (E) Average shortest path length of brain regions to the network core (rich club) is negatively correlated with global synchrony ($r = -0.74$; $P < 10^{-308}$), indicating that brain regions with a lower path length to the core are more likely to produce a coherent state.

with cognitive control and proposed to be complementary systems that may often need to process task-relevant information concurrently. Their dominance in producing metastable states likely reflects the fact that these systems can work in seclusion without coactivating a large part of the brain (facilitating parallel processing) and that they are flexible and not constrained by their structural connectivity. Both the auditory and ventral temporal association systems also contribute substantially to metastable states. These two systems are both predominantly located in the temporal lobe, an area of the brain associated with knowledge representation, so their functional roles may also frequently require working in seclusion in support of higher-order perception.

Although coherent and metastable states are dominantly produced by specific cognitive systems, all nine systems give rise to chimera states (Fig. 4B). Chimera states are more likely to occur than either coherent or metastable states (Figs. 2B and 3B), since they encompass a variety of different spatial patterns of coexisting coherent and incoherent behavior. This likely reflects the foundational role of partial synchrony in large-scale brain function. Cognitive tasks constantly require the intricate balance between segregated and integrated neural processing (*5*). The robust occurrence of chimera states following stimulation to each of the nine cognitive systems reflects the complexity and flexibility of the brain's underlying architecture to support diverse processing requirements. Although the distributions of states discussed above are obtained using a single threshold value ($\rho_{Th} = 0.8$), a qualitatively similar description can be obtained for a range of threshold values, as shown in figs. S5 and S6, indicating that our analysis is robust for cognitive interpretations.

Structural variability influences spatial patterning of observed emergent states

A major advantage of our approach is the ability to obtain the spatial patterns that comprise individual chimera states, which can then be interpreted within the cognitively informed framework to understand how structural constraints influence the large-scale functional organization of the brain. We next characterize this spatial patterning of emergent states to understand which cognitive systems are synchronized and desynchronized following stimulation to each region. The

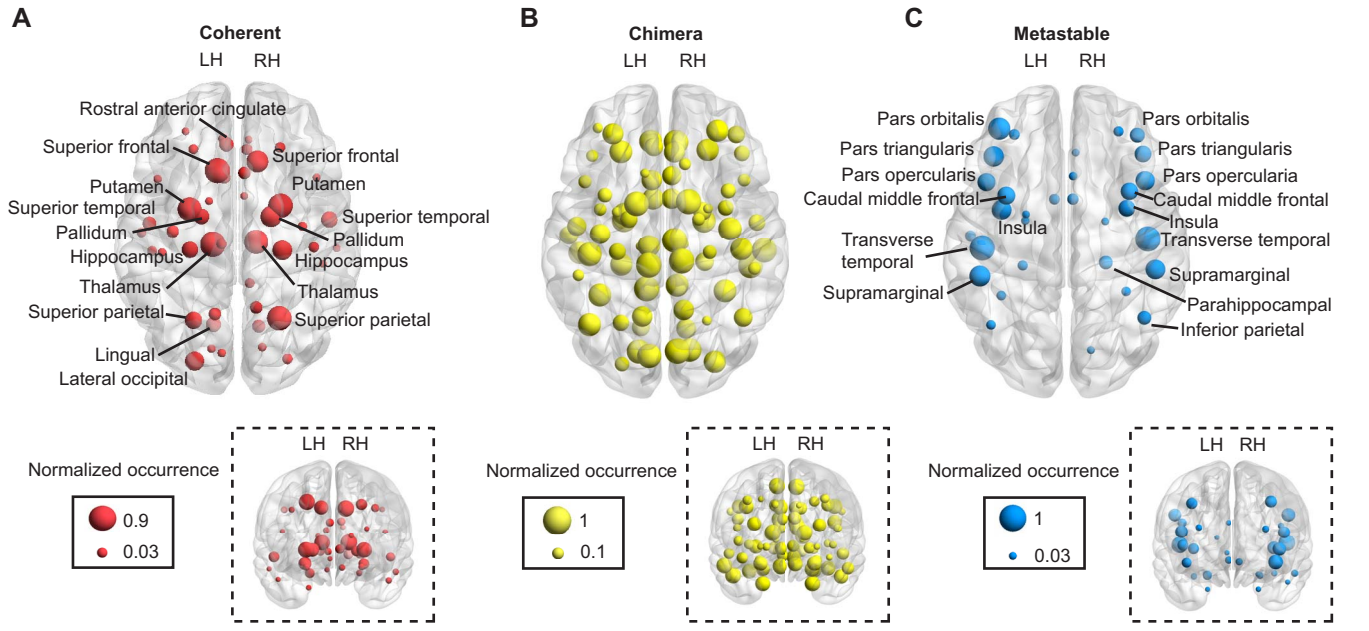

Fig. 3. Distributed origin of dynamical states. Separate depictions of brain network regions (nodes) that produce each of the three dynamical states: (**A**) coherent, (**B**) chimera, and (**C**) metastable. Both axial and coronal views of the brain are presented to visualize the anatomical location of the node in the left (LH) and right (RH) hemispheres. The radius of a node represents the normalized occurrence or likelihood of a given state upon stimulation of that node across all the individuals. As illustrated by the variability in node size, different states can emerge upon the stimulation of a single node across subjects, with larger nodes indicating that the region is more likely to consistently produce patterns of a given state. (A) While regions distributed throughout the brain are capable of producing a coherent state, the coherent state is relatively more likely to originate from the stimulation of nodes close to the midline of the brain. (B) Chimera states are likely to be originated by the stimulation of nodes that are relatively equally distributed within the brain; however, these nodes may vary in the spatial patterns of synchronization that they produce. (C) A metastable state is more likely to originate from the stimulation of brain regions away from the midline of the brain.

results are organized by stimulation of brain regions within a cognitive system in Fig. 5 (A to I), where each row is a pattern of synchronization within the nine cognitive systems. The rows are organized by the frequency with which the pattern was observed (listed to the right of the row) after stimulation to all regions within that system and across all individuals in the study. For each pattern, systems that are part of the synchronized population after stimulation are shown in orange, and systems that are part of the desynchronized population are shown in white. Consequently, coherent, metastable, and chimera states are demarcated by a fully orange row, a fully white row, and a mixed pattern of coloring, respectively. For each cognitive system (Fig. 5, A to I), we present the prevalent patterns observed (those that occur with a frequency of $\geq$3%), and these results illustrate what systems are likely to synchronize after stimulation.

Aligned with their complementary roles in cognitive control, the cingulo-opercular and frontoparietal systems continue to show similarity in their patterns of synchronization. The dominant pattern after stimulation to regions in either system is a metastable state, occurring 37% of the time for the cingulo-opercular system (Fig. 5C) and 42% of the time for the frontoparietal system (Fig. 5D). Similarly, the auditory system also produces a metastable state 50% of the time (Fig. 5B). For all three of these systems, the second most frequent state is the opposite extreme, a coherent state (20% for auditory and 10% for cingulo-opercular) or a nearly coherent state (9% for frontoparietal). Thus, these three systems show diversity in the types of dynamical states that they are capable of producing: Stimulation of some nodes within the system produces a metastable (segregated) state, while stimulation of others drives the brain to a coherent (integrated) state.

The ventral temporal association system also produces a metastable state as its most prevalent pattern (Fig. 5H), but unlike in the three previously discussed systems, this state is produced less frequently (11%), and the system also produces a much larger variety of prevalent patterns of synchronization (10 unique patterns). The only other system to show this high level of diversity in its produced patterns is the motor and somatosensory system (11 patterns; Fig. 5F). In both systems, we observe multiple patterns of chimera states. This likely reflects the ubiquitous need for neural processing related to both action coordination (motor and somatosensory) and higher-order perception (ventral temporal association) to be integrated with the processing occurring in other systems within the brain (*36*).

A coherent state occurs most frequently for the attention (41%; Fig. 5A), default mode (31%; Fig. 5E), and subcortical systems (44%; Fig. 5G). The visual system is also similar, although the coherent state is the second most prevalent (21%), with a nearly coherent state (all but auditory) as its dominant pattern (23%). Overall, these four systems seem relatively less dynamically diverse since their stimulation largely results in chimera states with high synchrony. All of these systems serve fundamental functional roles to rapidly respond to the external environment, and their dynamical patterns reflect this need to efficiently integrate this information with other cognitive systems.

For all systems, the most common state following regional stimulation is a chimera state with high synchrony, emphasizing the importance of partial synchrony for all of the diverse functional roles provided by large-scale cognitive systems. Visual inspection of the patterns suggests that the systems most likely to belong to the desynchronized population of a chimera state are the three systems that

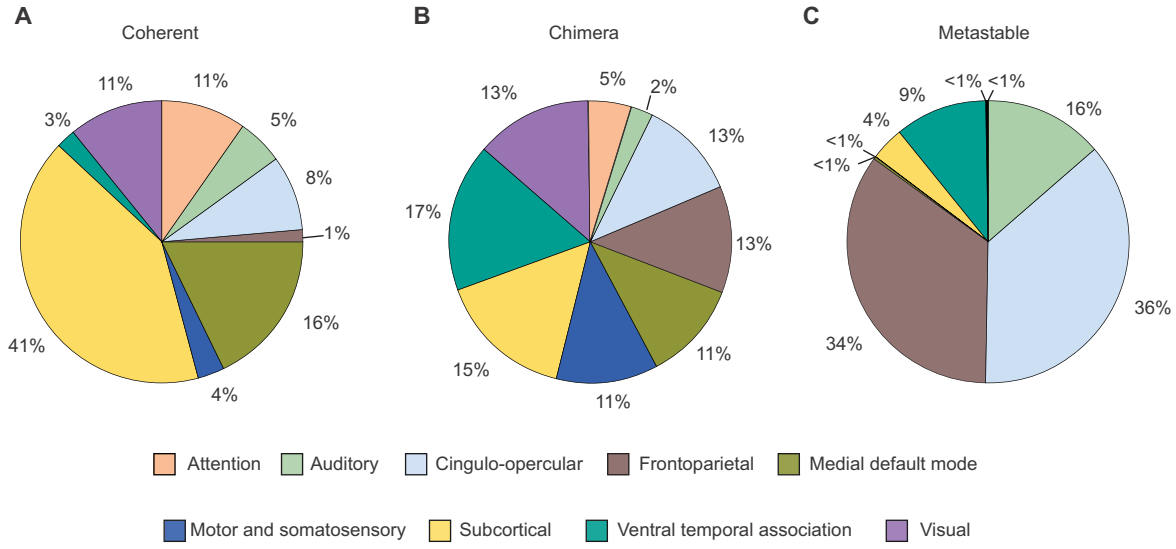

Fig. 4. Contribution of cognitive systems to dynamical states. (**A**) Coherent states are likely to result when nodes within the medial default mode and subcortical systems are stimulated. (**B**) Chimera states emerge upon the stimulation of nodes that are equally distributed across all the cognitive systems. (**C**) Metastable states frequently occur after stimulation of nodes within auditory, cingulo-opercular, frontoparietal, and ventral temporal association systems. This distribution indicates the dominance of a particular type of cognitive role within the nodes of different cognitive systems.

predominantly produce a metastable state (auditory, cingulo-opercular, and frontoparietal systems). We quantify this effect in the synchronization probability plot (Fig. 5J). Systems with a high probability of synchronization have dark colors, while systems that are unlikely to be synchronized as a result of stimulation to a specific cognitive system are shown in light colors. While the auditory, cingulo-opercular, and frontoparietal systems are all unlikely to synchronize with other systems, the attention system, in contrast, is highly likely to be part of the synchronized population following stimulation to any system. We also observe that the stimulation of a region within a particular system does not necessarily induce synchronization within that system, which is particularly the case with the auditory, cingulo-opercular, and frontoparietal systems.

Thus far, following the cognitively informed architecture of the system-level brain partitioning, we have argued that the different patterning of states within a system reflects a link between cognitive processing and the structural constraints of each system. Computationally, however, any coarse partitioning of the brain network could result in the emergence of a variety of states, including chimeras, upon regional stimulation. Note that the general emergence of chimera states is not unique to the brain partitioning we have used. However, what is unique are the characteristically distinct patternings of the individual chimera states that emerge, and it is the specific combination of cognitive systems that synchronize in a given chimera state that provides a unique neuroscientific relevance to our framework. Our decision to partition the brain based on cognitive system assignments therefore provides a necessary and specific interpretation framework.

To support this argument, we compared our results to those obtained using a random partitioning of the brain into nine groups (equivalent to systems). In randomized partitioning, we used the same number of regions within a group as in our original analysis, but brain regions were randomly assigned to these groups (see Materials and Methods for details of the randomization). We next performed two different randomization experiments. In the first experiment, we created a single randomized partition of the brain and applied our analysis across all 30 subjects (fig. S7A). In the second experiment, we created 10 different random partitions of the brain and performed our analysis for each of the 10 partitions across all 30 subjects and extracted the prevalent patterns (those that occur with a frequency of $\geq$3%) produced from this larger ensemble (fig. S7B). The first experiment using a single random partition across subjects reveals that the general emergence of chimera states is not unique to the cognitively informed partitioning of the brain, as applying a random partition can also produce chimera states. However, the second experiment shows that the patterning of chimera states produced by applying a random partition of the brain is dependent on the specific configuration of the partition; the coherent and metastable states dominate the prevalent patterns. This represents the fact that each random partition of the brain produces a different set of chimera patterns such that there is little chance that any given pattern will appear as a prevalent pattern.

Note that, in both randomization experiments, the top two prevalent states are the coherent and metastable states. This is different from the results shown in Fig. 5, where system assignments are based on a region's cognitive system assignment and spatially distinct patterns of partial synchrony (chimera states) appeared in the top two prevalent patterns in certain systems. This finding highlights the importance of uniting a cognitive systems framework with a chimera-based analysis to understand and interpret the emergent patterns of synchronization in the brain. Within a cognitive framework, a similarity in chimera states across subjects may reveal the link between structural constraints and functional patterns that support human cognition.

Collectively, these results reveal the power of our approach to characterize and understand structural constraints to the large-scale system interactions after regional stimulation. In fig. S8, we further describe how different regions in a system contribute to observed patterns by spatially mapping the probability of a given pattern onto the brain. Together, these results highlight that stimulation within each system gives rise to multiple patterns, similar patterns can emerge from spatially different regions, and within a system, there can be a special distribution of states across brain regions. This likely arises from individual

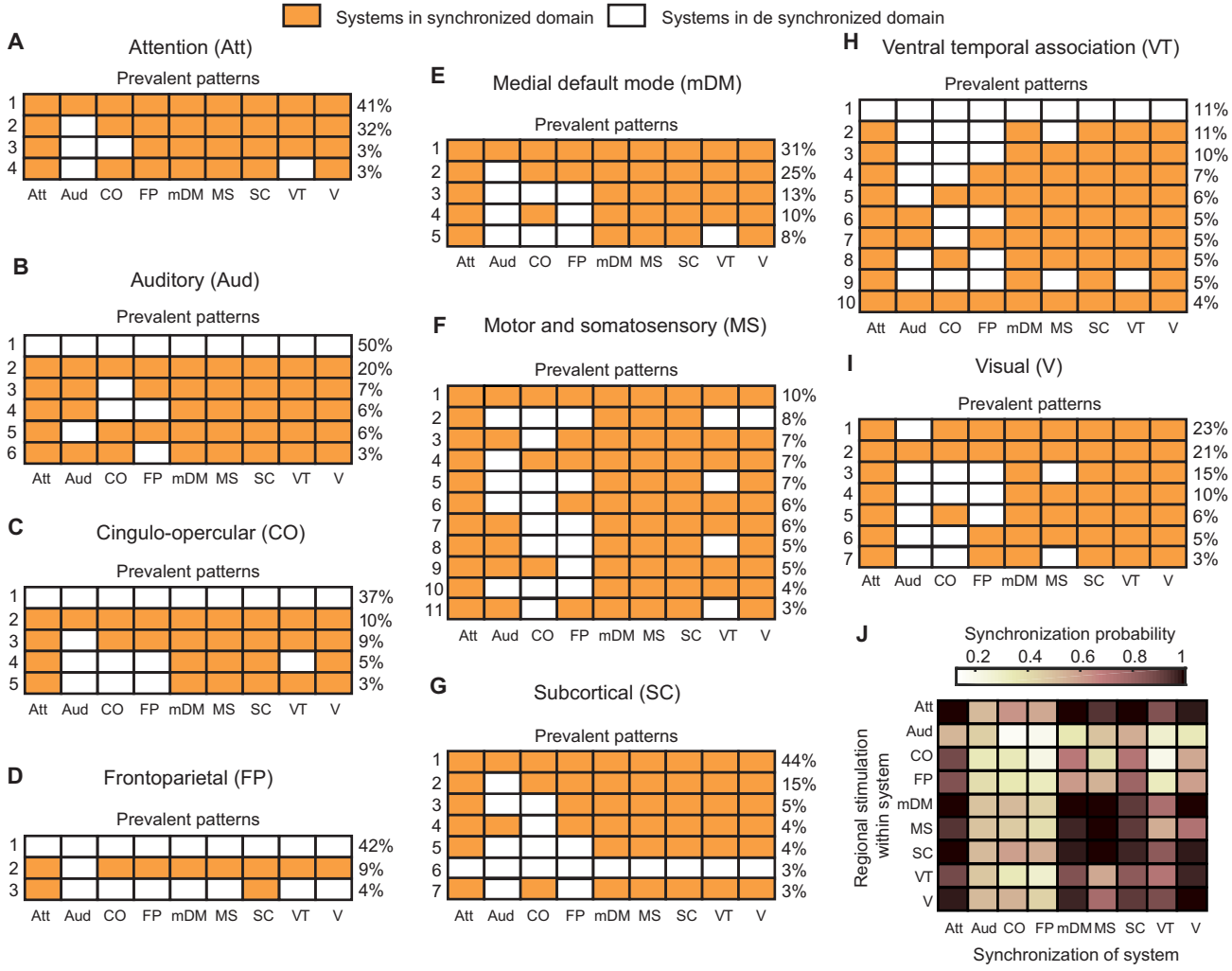

Fig. 5. Patterns of synchronization and cognitive chimera states. (**A** to **I**) Prevalent patterns of synchrony that emerge as regions within different cognitive systems are stimulated across all subjects. When brain regions were stimulated both within a given cognitive system and across all subjects, different patterns of synchronization emerged. Some of the patterns were found to be repeated for different regions and/or subjects, while some occurred occasionally. If the same pattern occurred when each brain region within a cognitive system was stimulated and if this was true across all 30 subjects, then the pattern would have a frequency of 100%. Here, we show patterns that occurred at least 3% of the time for stimulation of brain regions within a cognitive system across all subjects. Each panel represents stimulation of regions within a particular cognitive system. Each row represents one pattern of synchronization, and each column represents the state of a cognitive system. Cognitive systems that belong to the synchronized population are colored orange, and cognitive systems that remain desynchronized are colored white. Thus, a fully orange or white row represents a coherent or metastable state, respectively. Chimera states show different patterns of coloring depending on the cognitive systems that are recruited to the synchronized group. Different rows of patterns are stacked on the basis of their relative occurrences (mentioned on the right side). To summarize the observed patterns, (**J**) The probability with which different cognitive systems can be synchronized when the regions within a given system are stimulated across subjects (shown along the vertical axis).

differences in the structural connectivity between the participants in the study or differences in the structural connectivity of the regions themselves within each system (or a combination of the two). Consequently, we introduce a new metric to assess the contribution of subject-specific and region-specific variability on the observed patterns.

Dissociation of subject-specific and region-specific variability

In our final analysis, we compute a measure called robustness, which we defined to quantify the level of similarity between a set of observed patterns (see Materials and Methods) to assess how structural variability, either between subjects or between regions, influenced the patterns observed in Fig. 5. To differentiate these two potential sources of variability, we separately compute a subject robustness and a region robustness score (see Materials and Methods). When robustness is calculated across individuals (subject robustness), it measures the similarity of different patterns produced across individuals by stimulating the same brain region. A cognitive system's subject robustness is then the average subject robustness across regions within the system. When robustness is calculated across brain regions (region robustness), it measures the similarity of different patterns produced by stimulation of different brain regions within a given cognitive system in a single subject. This value is then averaged over all subjects. Consequently, a high value of robustness indicates a high similarity between synchronization patterns produced by stimulation across individuals (subject robustness) or brain regions (region robustness).

In Fig. 6, we plot each cognitive system based on its score for subject robustness and region robustness. In addition, we group cognitive systems by applying a clustering algorithm (see Materials and Methods), and the color and shape of a system's icon reflects its group assignment. We identify four distinct groups of systems that are characteristically different from each other in terms of their location in the robustness space and also in their cognitive roles. To better delineate the four groups, we partition the robustness space based on the level of subject and node robustness. We define two levels of subject robustness—variable and stable—while the node robustness is partitioned into three levels—diverse, flexible, and consistent.

Across the subject robustness dimension, we observe four individually variable systems that demonstrate the largest variability in patterns. These systems include the frontoparietal and cingulo-opercular, the cognitive control systems that have previously been shown to have large individual variability (*37*), and ventral temporal association and motor and somatosensory systems that show learning-dependent changes (*36*, *38*). The remaining five systems are classified as individually stable with high subject robustness scores. The default mode, subcortical, and attention systems have previously been found to be preserved across individuals and across species (*39*), whereas the auditory and visual systems support fundamental perceptual processing (*40*).

Across the region robustness dimension, we observe three levels of robustness. Cognitively consistent groups include the attention and subcortical systems, indicating that stimulation to regions within these systems give rise to similar patterns of synchrony and desynchrony. The auditory system emerges as the sole cognitively diverse system. This reflects the starkly different patterns that arise after stimulation of the regions within this system. For example, stimulation to the superior temporal region results in high-synchrony states (both coherent and chimera), while stimulation to the transverse temporal region leads to a metastable state (see fig. S8). Thus, the different local connectivity patterns of regions within this system produce immense diversity in the resulting synchrony patterns upon their stimulation. The remaining six cognitive systems are classified as cognitively flexible, indicating that stimulation of regions within these systems produced variable patterns of synchrony.

Overall, the robustness scores both confirm and extend our knowledge of brain structure-function relationships. The variability in subject robustness among the systems reflects known differences in system stability between individuals and confirms that variability in chimera patterns captures these coarse differences among the systems. On the other hand, the spread of region robustness scores captures the diversity in the functional roles that the regions within a system serve across diverse cognitive tasks. Cognitively consistent systems can largely be involved in core sensory processing and associative learning, whereas the variability of patterns within cognitively flexible systems may enable them to serve diverse cognitive roles, relying on stimulation of each constituent as a means to synchronize and integrate with different cognitive systems to support particular cognitive demand or task-relevant processing.

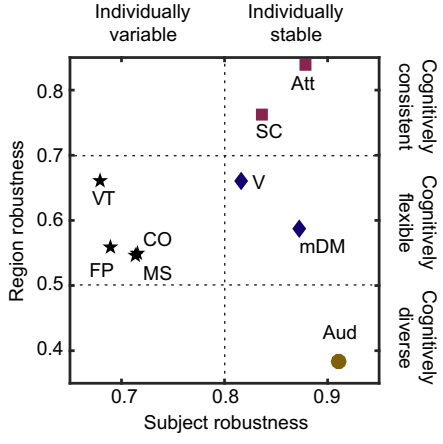

Fig. 6. Classification of cognitive systems based on pattern robustness. To estimate the consistency of emergent patterns of synchronization within cognitive systems, we constructed a measure called robustness that estimates the similarity between a set of patterns. Within a cognitive system, we calculate robustness across two dimensions: patterns that are produced after stimulating each region across subjects (subject robustness) and patterns that are produced after stimulating different regions of the system within each subject (region robustness). In the parameter space constructed along these dimensions, we can cluster cognitive systems into four groups that suggest a 2 by 3 partitioning of the robustness space. This partitioning allows us to dissociate subject-specific and region-specific variability in observed patterns.

DISCUSSION

Using a novel, chimera-based framework, we explored the dynamical states that emerge across large-scale cognitive systems following the spread of a targeted regional stimulation. We identified three distinct dynamical states—coherent, chimera, and metastable—that arise as a function of the structural connectivity of the stimulated regions. A core result across all analyses is the variety in frequency and distribution of the observed dynamical states. Chimera states are the most pervasive state to emerge following regional stimulation. This likely reflects the foundational role that partial synchrony serves in large-scale brain function to enable the intricate balance between segregated and integrated neural processing. Furthermore, the diversity in these patterns captured both subject- and region-specific variability in structural connectivity. On the basis of its sensitivity to these different sources of variability, our novel chimera-based framework shows immense promise to better understand individual differences, relate patterns to performance, and understand system constraints that underlie how to drive the brain to different task-relevant states.

Prevalence of chimera states across cognitive systems enables segregation and integration in brain dynamics

The brain is a complex dynamical system that must integrate information across spatially distributed, segregated regions that serve specialized functional roles (*41*). Neuroscience research therefore attempts to understand how the brain creates selective synchrony across subsets of task-relevant regions to enable rapid and adaptive cognitive processing. Recently, network neuroscience approaches have identified sets of brain regions that form cognitive systems during rest and task states (*42*). By studying the interactions of these cognitive systems, functional analyses have identified the importance of (i) integrated states where the connections are stronger between cognitive systems (*5*) and (ii) segregated states where connections are weaker between cognitive systems and are likely to be stronger within. The relative level of functional integration versus segregation of cognitive systems has important consequences for cognitive performance. Highly segregated systems enable efficient computations in local, functionally specialized brain regions, while strongly integrated systems provide rapid consolidation of information across systems necessary for coordinated,

cohesive performance of complex tasks (*5*). These crucial brain states are captured in the present framework as metastable (segregated) and coherent (integrated) states and, perhaps the most critical for brain function, as the chimera state that describes partial synchrony across subsets of cognitive systems.

All nine systems give rise to a chimera state following stimulation, suggesting that all cognitive systems can drive the brain to partial synchrony in support of their functional roles in cognition. Our results augment a burgeoning literature on how brain dynamics support rapid shifts between more segregated or integrated brain states. Previous work has found that functionally segregated states tend to involve shorter, local connections (*43*), while integration largely relies on the global influence of subcortical regions and cortical hubs that have many diverse connections to other brain regions (*44*). Collectively, our results demonstrate that our novel chimera framework can investigate critical cognitive states where a balance between integration and segregation is required for adaptive cognition.

Chimera framework reveals subject-specific and region-specific variability in brain connectivity through the analyses of emergent dynamical states

We found that a coherent state is likely to be produced by the stimulation of regions in the medial default mode and subcortical systems. This reflects the propensity of these systems to contain regional hubs, and the prevalent emergence of a coherent state reflects their functional roles to bridge spatially disperse regions and facilitate global brain communication. These systems also have high subject robustness, indicating robust occurrence of patterns across the 30 individuals. This could reflect that the subcortical and medial default mode systems provide a fundamental, constant pillar of brain organization, which when disrupted, could lead to impairments in global brain function. Previous research has shown that network hubs are often found to be affected in neurological disorders such as schizophrenia and Alzheimer's disease (*45*). These disorders are associated with network-wide deficits in brain function (*21*), which is consistent with our finding that cognitive systems that produce coherent states also contain network hubs.

Conversely, metastable states are preferentially produced by four systems with more sparse structural connectivity: two systems associated with cognitive control (cingulo-opercular and frontoparietal systems) and two systems associated with intricate sensory, object, and language representations (auditory and ventral temporal association systems). These systems all have functional roles that frequently require working in seclusion from other specialized processing in the brain. The three systems that are the most unlikely be synchronized upon stimulation are also the ones that are most likely to produce a metastable state: the auditory, cingulo-opercular, and frontoparietal systems. The cingulo-opercular and frontoparietal systems are associated with cognitive control, and they are proposed as complementary systems that are specialized for guiding successful task performance at different timescales: the cingulo-opercular system for maintaining task-related goals across trials and the frontoparietal systems for trial-by-trial control (*46*). These functional roles may often need to occur concurrently, and their production of metastable states could indicate that these systems can work in seclusion without coactivating a large part of the brain, an attribute that facilitates parallel processing.

While our chimera framework revealed stable features of brain architecture, it also captured cognitive systems where between-subject variability leads to variety in frequency and type of synchronization patterns: cingulo-opercular, frontoparietal, ventral temporal association, and motor systems. These four systems with low subject robustness are associated with higher cognitive functions where an individual's experience and knowledge are likely captured by variability in their structural connectivity (*47*). Our results demonstrated that the frontoparietal and cingulo-opercular systems exhibit a very strong individual variability, and this mirrors recent results that showed that cognitive control systems have weaker within-subject variability and greater between-subject variability relative to sensory processing systems (*37*). Our results also demonstrated that the ventral temporal association and motor and somatosensory systems show an especially high number of prevalent patterns with no single dominant pattern, and this may reflect their roles in learning and development-related changes (*38*).

Beyond the present framework and future directions

Our model is only sensitive to functional relationships that are induced through structural connections, so the observed dynamical states and patterns are only constrained by the anatomical structure of the network. Here, the emergence of a coherent pattern would imply that a region can, in principle, communicate with all of the spatially distributed regions within the brain; however, the actual regions that it communicates with may vary between different tasks according to the specific cognitive demands of the task. Nevertheless, we have recently shown that, by quantifying differences in the structurally constrained patterns of in silico brain activity resulting from regional stimulation, one can explain individual variability in performance of tasks that differ in cognitive complexity (*26*).

In reality, neuronal activity patterns that are observed in the brain using different functional measurement techniques, such as functional magnetic resonance imaging (MRI), electroencephalography, magnetoencephalography, and positron emission tomography, are a result of a complex neurophysiological activity that develops on top of the structural connectivity infrastructure. Thus, the actual patterns of brain activity that are observed across functional modalities may come from the simultaneous activation of different brain regions via multiple input sources and therefore might differ from the patterns observed in our in silico experiments. However, our computational approach can still aid in the conception of cognitive hypotheses and experimental design. The framework allows us to evaluate the patterns of activity resulting from the activation of a specific cognitive system to understand the variety of cognitive roles it could play, and thus, its use extends beyond making overall comparisons between the characteristic patterns of synchrony across cognitive systems. For example, the dominance of high-synchrony patterns upon stimulation of brain regions within the default mode system (Fig. 5E) could indicate its important role in resting-state dynamics and ability to switch communication between brain regions when the brain changes state from rest to task performance. In contrast, the emergence of low-synchrony states (Fig. 5E) could indicate the involvement of the default mode system in specific cognitive control roles. Recent findings have suggested task-related changes in the topography of the default mode system (*48*, *49*).

Last, the emergence of a metastable state may not reflect the absence of synchrony in the entire population. A stable synchronization could potentially exist within a population substantially smaller than our spatial resolution, and future research can investigate effect of scale using models at a finer spatial resolution. Despite these limitations, our approach is sensitive to variability in region-specific and subject-specific brain connectivity, and it can be used to answer fundamental questions

concerning the cognitive organization of the human brain. Future research can extend our in silico experiments to examine chimera states using experimental data, providing opportunities to enhance performance in healthy participants or individualize medicine in clinical populations. More generally, this approach provides an opportunity to establish a connection between the structure of an individual's brain network and cognitive performance (*26*).

CONCLUSION

Using the cognitive system framework (*28*), our novel chimera-based approach reveals specific features (spatial structure and prevalence) of interaction patterns among large-scale cognitive systems in the human brain. These features provide insight into how structural constraints within cognitive systems are linked to patterns of brain activity that reflect the systems' ability to perform a variety of cognitive tasks. The spatial patterns of partial synchrony within chimera states observed in this study have a natural link to the well-documented role of functional segregation and integration of cognitive systems thought to support cognition (*6*), and the approach is capable of extracting robust system differences for those that are largely stable across people and those that capture individual training and expertise. Thus, our approach provides a rich opportunity to study how dynamical states give rise to variability in cognitive performance, providing the first conceptual framework to understand how chimera states may subserve human behavior.

MATERIALS AND METHODS

Experimental design

Diffusion MRI analysis was performed on the 30 individual participant scans previously reported elsewhere (*50*). Twenty male and 10 female participants were recruited from Pittsburgh and the Army Research Laboratory in Aberdeen, Maryland. All participants were neurologically healthy, with no history of either head trauma or neurological or psychiatric illness. Participant ages ranged from 21 to 45 years at the time of scanning (mean age of 31 years), and four were left-handed (two males and two females). All participants signed an informed consent approved by Carnegie Mellon University and conforming with the Declaration of Helsinki and were financially remunerated for their participation.

Macroscopic white matter pathways were imaged using a DSI acquisition sequence on a Siemens Verio 3T MRI system located at the Scientific Imaging and Brain Research Center at Carnegie Mellon University using a 32-channel head coil. A total of 257 directions was sampled using a twice-refocused spin-echo sequence (51 slices; repetition time (TR), 9.916 s; echo time (TE), 157 ms; 2.4 mm by 2.4 mm by 2.4 mm voxels; 231 mm by 231 mm field of view (FoV); maximum b-value 5000 s/mm^2). Diffusion data were reconstructed using *q*-space diffeomorphic reconstruction (*51*) with a diffusion sampling length ratio of 1.25 and an output resolution of 2 mm.

Construction of individual structural brain networks

Whole-brain structural connectivity matrices were constructed for each individual (subject) using a bootstrapping approach. To minimize the impact of bias in the tractography parameter scheme on streamline generation, whole-brain fiber tractography (*52*) was performed 100 times for each participant, generating 250,000 streamlines per iteration. Across the 100 iterations, values were randomly sampled for quantitative anisotropy based fiber termination thresholds (0.01 to 0.10), turning angle thresholds (40 to 80), and smoothing (50 to 80%), while constant values were used for step size (1 mm) and minimum/maximum fiber length thresholds (10 mm/400 mm). On each iteration, a binary connectivity matrix was generated, where an edge between two regions of interest was considered present if 5% or more of streamlines generated were found to connect them. The probability of observing a connection was estimated by calculating the frequency of detecting an edge across all 100 iterations. The regions of interest were determined using cortical components of the Desikan-Killiany atlas and subcortical components of the Harvard-Oxford subcortical atlas. In the resulting weighted matrices, connection strengths were normalized by the sum of the regional brain volumes, and these normalized matrices were used as the structural representations of individual brains. All analyses were performed using DSI Studio (http://dsi-studio.labsolver.org/) and MATLAB (MathWorks Inc., Natick, MA, USA).

Data-driven network model of brain dynamics

In our data-driven network model, regional brain dynamics were given by WCOs (*26*, *27*, *29*). In this biologically motivated neural mass model, the fraction of excitatory and inhibitory neurons active at time t in the ith brain region are denoted by $E_i(t)$ and $I_i(t)$, respectively, and their temporal dynamics are given by

$$\tau\frac{dE_i}{dt} = -E_i(t) + (S_{E_m} - E_i(t)) \times S_E\left(c_1E_i(t) - c_2I_i(t) + c_5\sum_j A_{ij}E_j(t-\tau_d^{ij}) + P_i(t)\right) + \sigma w_i(t) \quad (1)$$

$$\tau\frac{dI_i}{dt} = -I_i(t) + (S_{I_m} - I_i(t)) \times S_I\left(c_3E_i(t) - c_4I_i(t) + c_6\sum_j A_{ij}I_j(t-\tau_d^{ij})\right) + \sigma v_i(t) \quad (2)$$

where

$$S_{E,I}(x) = \frac{1}{1+e^{-a_{E,I}(x-\theta_{E,I})}} - \frac{1}{1+e^{a_{E,I}\theta_{E,I}}} \quad (3)$$

A_{ij} is an element of the subject-specific coupling matrix A whose value is the connection strength between brain regions i and j as determined from DSI, as described above. The global strength of coupling between brain regions was tuned by excitatory and inhibitory coupling parameters c_5 and c_6, respectively. In this case, $c_6 = c_5/4$. $P_i(t)$ represents the external stimulation to excitatory-state activity and was used to perform computational stimulation experiments. The parameter τ_d^{ij} represents the communication delay between regions i and j. If the spatial distance between regions i and j is d_{ij}, then $\tau_d^{ij} = d_{ij}/t_d$, where $t_d = 10$ m/s is the signal transmission velocity. We added noise as an input to the system through the parameters $w_i(t)$ and $v_i(t)$, which were derived from a normal distribution with $\sigma = 0.00005$. Other constants in the model were biologically derived: $c_1 = 16$, $c_2 = 12$, $c_3 = 15$, $c_4 = 3$, $a_E = 1.3$, $a_I = 2$, $\theta_E = 4$, $\theta_I = 3.7$, and $\tau = 8$, as described in (*26*, *27*, *29*). To numerically simulate the dynamics of the system, we used a stochastic Euler-Maruyama method with step size of 0.01 ms with initial conditions $[E_i(0), I_i(0) = 0.1, 0.1]$.

Targeted stimulation

The model was optimized for each individual to allow a regime of maximum dynamical sensitivity. This was performed by choosing a

global coupling parameter, c_5, such that the system was just below the critical transition point to the excited state (see fig. S1). Regional stimulation was achieved by applying a constant external input $P_i = 1.15$ to a single region and perturbing its dynamics (fig. S1). As the dynamics evolve, the stimulation spreads within the brain through the network connectivity of the stimulated node.

Cognitive systems

We assigned each brain region to one of nine cognitive systems: attention, auditory, cingulo-opercular, frontoparietal, medial default mode, motor and somatosensory, subcortical, ventral temporal association, and visual. This node assignment is described in table S1 and is similar to the one used by Muldoon *et al.* (*27*). The distribution of brain regions within cognitive systems is shown in fig. S2.

Calculation of synchronization within cognitively informed framework

We used the standard order parameter ρ to estimate the extent of synchronization after a targeted regional stimulation within the brain networks. This measure was proposed by Kuramoto for the estimation of coherence in a population of Kuramoto phase oscillators (*33*). In this case, the instantaneous order parameter at a given time t was defined as

$$\rho_N(t)e^{i\Phi(t)} = \frac{1}{N}\sum_{j=1}^{N} e^{i\phi_j(t)} \quad (4)$$

where ϕ_j is the phase of the jth oscillator at time t and is given by

$$\phi_j(t) = \tan^{-1}\frac{I_j(t)}{E_j(t)} \quad (5)$$

Here, $N = 76$ is the number of oscillators in the system. To estimate the global synchronization in the system, one needs to average the instantaneous order parameter for a sufficiently long period of time (T).

$$\rho_N = <\rho_N(t)>_T \quad (6)$$

We used 1 s of simulated activity to estimate the average order parameter. Within our cognitively informed framework, we measured the synchronization between all pairs of cognitive systems following a regional stimulation. This was performed by calculating an order parameter for the combined oscillator population of a pair of cognitive systems. For cognitive systems s_i and s_j, this order parameter is given by

$$\rho_{s_i,s_j} = <\rho_{s_i,s_j}(t)>_T \quad (7)$$

where

$$\rho_{s_i,s_j}(t)e^{i\Theta(t)} = \frac{1}{N_{s_i}+N_{s_j}}\sum_{k\in(s_i\cup s_j)} e^{i\phi_k(t)} \quad (8)$$

Here, N_{s_i} and N_{s_j} represent the number of oscillators (brain regions or nodes) within cognitive systems s_i and s_j, respectively. This analysis resulted in synchronization matrices, as shown in Fig. 2A, whose entries represent the extent of synchronization between cognitive systems. These matrices were used to identify the dynamical cognitive state that emerged as a result of regional stimulation.

Chimera index and metastability index

We calculated the chimera index, C, and metastability index, λ, as described in (*24*, *34*). C is a measure of the normalized average variation in the order parameter within cognitive systems averaged over time. For $s_i \in [s_1, s_2, \ldots, s_M]$ ($M = 9$ is the total number of systems)

$$C = \frac{<\sigma_{ch}(t)>_T}{C_{Max}} \quad (9)$$

where

$$\sigma_{ch}(t) = \frac{1}{M-1}\sum_{i=1}^{M}(\rho_{s_i}(t) - <\rho_s(t)>_M)^2 \quad (10)$$

In this case, $C_{Max} = 5/36$ is a normalization factor and represents the maximum value of variability in the order parameter in an ideal chimera state where the network organizes such that the half of its population is completely synchronized and half is completely desynchronized (*34*). The instantaneous quantity $<\rho_s(t)>_M$ measures the synchronization of cognitive systems, averaged over all systems at a given time t.

Similarly, λ measures the normalized temporal variation of the order parameter averaged across all cognitive systems

$$\lambda = \frac{<\sigma_{met}(s)>_M}{\lambda_{Max}} \quad (11)$$

where

$$\sigma_{met}(s) = \frac{1}{T-1}\sum_{t\le T}(\rho_{s_i}(t) - <\rho_{s_i}>_T)^2 \quad (12)$$

Here, $\lambda_{Max} = 1/12$ is a normalization factor (*34*), representing the scenario where the system spends equal time in all stages of synchronization.

Extraction of the patterns of synchronization

To identify emergent cognitive patterns, we first obtained a binarized synchronization matrix (m) such that $m_{ij} = 1$ if systems i and j are identified as synchronized and $m_{ij} = 0$ otherwise. We defined two cognitive systems s_i and s_j to be synchronized if $\rho_{si,sj} \ge \rho_{Th}$, where ρ_{Th} represents a synchronization threshold. For the results discussed throughout the main text, we used $\rho_{Th} = 0.8$ (*33*) (as indicated in Fig. 2A).

In principle, one can directly use these binarized synchronization matrices to classify the emergent states and patterns. However, we performed community detection on these binarized matrices. This method clusters the group of synchronized systems into a single community, whereas desynchronized systems remain as separate communities. In case of a coherent state, we observed only one community, and in case of a metastable state, we observed nine separate communities, each representing a cognitive system. For chimera states, communities with different distributions of cognitive systems emerged. Thus, applying the community detection algorithm not only allowed us to robustly

classify the emergent dynamical states but also let us separate various spatially distributed patterns of chimera states. Community detection was performed using modularity maximization through the generalized Louvain algorithm (*53*). For community detection, the value of the resolution parameter was varied between 0.8 and 0.95, and a consensus was run to determine the community structure (*54*).

Network connectivity features

Weighted degree and ranking

The weighted degree (W_i) of a brain region or node i is defined as $\sum_j A_{ij}$, and the distribution of weighted degrees typically varies across subjects. Therefore, to be able to compare weighted degrees across subjects, we ranked each node within a subject such that the higher value of the node rank signifies the higher value of its weighted degree. Similar rankings were obtained for each node for the amount of global synchrony and chimera index it produced upon stimulation.

Rich club analysis

A set of core nodes was defined such that the brain network can be partitioned into two separate groups with one group consisting of highly connected hubs (core) and the other group composed of peripheral nodes with low intragroup connectivity. We used the Brain Connectivity Toolbox (*55*) to obtain a set of core nodes for each subject (brain network). To define a set of core regions, we used a range of thresholds (0.5 to 1.5; a lower value of this threshold allows a higher number of nodes to be classified as the core). We then identified the regions that were assigned to the core across the entire range of thresholds, and these nodes where chosen to form the core of given subject. Then, we obtained the average shortest path length to the core for each brain region i, within each subject using the following steps: (i) calculating the average of the shortest path lengths between node i and the group of core nodes ($D_i^{\text{sub}} = < D_{ij}^{\text{sub}} >_j$, $j \in$ Core) and (ii) normalizing D_i^{sub} by maximum of D_i^{sub} in a subject. The shortest path length between two nodes was calculated with the Brain Connectivity Toolbox (*55*), and it represents the smallest path through network edges that connects those nodes.

Randomizing brain network partitioning

To assess the importance of a cognitively informed framework, we obtained the patterns of synchronization when the brain was randomly partitioned into nine different groups (systems). To obtain a random partition of the brain, we fixed the number of regions in each group to match their sizes with the original cognitively informed partitioning (systems 1 to 9 were 4, 4, 12, 10, 8, 6, 14, 10, and 8 regions per system, respectively) and then randomly assigned brain regions to each of these groups. We then used the previously simulated brain activity for each subject to calculate the system-level Kuramoto parameter, system-level synchronization matrices, and the patterns of synchrony (as described above) based on the new random partitioning of the brain. In the first randomization experiment, a single random partition was created and applied across all 30 subjects to extract the prevalent patterns (those that occur with a frequency of $\geq$3%) for each group. In the second randomization experiment, 10 different random partitions were created, and each partition was applied across all 30 subjects to extract the prevalent patterns from this larger ensemble.

Pattern robustness

A pattern in our analysis describes whether the given cognitive system falls into the synchronized population or remains desynchronized (Fig. 5). To calculate similarity between patterns, we defined the robustness of a set of observed patterns as follows

$$R = \frac{1}{p(p-1)} \sum_{i,j=1}^{p} \left(\frac{1}{M} \sum_{s=1}^{M} \delta_{i,j}^{s} \right) \quad (13)$$

where p is the number of patterns in the set. $\delta_{i,j}^{s} = 1$ if the cognitive system, s, falls into the same state of either synchrony or desynchrony in patterns i and j, and $\delta_{i,j}^{s} = 0$ otherwise.

We calculated the robustness of cognitive systems in two dimensions: across individuals for a given brain region within the system (subject robustness) and across regions of the system in a given subject (region robustness). For subject robustness of a given cognitive system, p constitutes the patterns that are produced by a given node for all the subjects and equals the number of subjects, i.e., 30. For region robustness of a given cognitive system, p constitutes the patterns that all the nodes for a given cognitive system produce for a given subject, and the value of p varies between systems. Thus, for each cognitive system, we obtained two distributions of robustness, one for each subject and region.

Clustering of cognitive systems using robustness features

In the subject-region robustness parameter space, we grouped cognitive systems into clusters using the k-means algorithm and silhouette analysis. We used k = 3, 4, 5, and 6 and identified the stable clustering that maximizes similarity within clusters and dissimilarity across clusters. One can obtain different clusterings of data based on the k value (number of clusters), and the silhouette value assesses the quality of the clustering. A value close to 1 signifies optimal clustering, meaning that the data points are more distant (defined by the Euclidean distance) from other clusters as compared to their own cluster, while a negative value signifies the opposite. Thus, if a_i denotes the average distance of a data point i from the data points in its own cluster and b_i denotes the average distance from the data points in other clusters, then the silhouette value is given by $S_i = (b_i - a_i)/\max(a_i, b_i)$. For k = 4, we observed an optimized clustering. The corresponding silhouette plot is shown in fig. S9.

Rendering of brain images

BrainNet Viewer was used to perform spatial mapping onto brain images (*56*).

Statistical analysis

All correlations in the manuscript were computed using the standard Pearson's correlation and deemed significant if $P < 0.05$.

SUPPLEMENTARY MATERIALS

Supplementary material for this article is available at http://advances.sciencemag.org/cgi/content/full/5/4/eaau8535/DC1

Fig. S1. Optimizing personalized BNMs and applying targeted regional stimulation.
Fig. S2. Distribution of brain volume within cognitive systems.
Fig. S3. Metastable state and metastability index.
Fig. S4. Relation between connectivity, position, and emergent cognitive state.
Fig. S5. Effect of changing synchronization threshold on the distribution of states.
Fig. S6. Likelihood of the emergence of dynamical states across cognitive systems.
Fig. S7. Patterns of synchrony for randomly partitioned brain networks.
Fig. S8. Normalized contribution of brain regions to the prevalent patterns of synchronization.
Fig. S9. Clustering of cognitive systems using pattern robustness.
Table S1. Assignment of brain regions to cognitive systems.

REFERENCES AND NOTES

1. A. Pikovsky, M. Rosenblum, J. Kurths, *Synchronization: A Universal Concept in Nonlinear Sciences* (Cambridge Univ. Press, 2001).
2. M. A. Bertolero, B. T. T. Yeo, M. D'Esposito, The modular and integrative functional architecture of the human brain. *Proc. Natl. Acad. Sci. U.S.A.* **112**, E6798–E6807 (2015).
3. L. M. Pecora, F. Sorrentino, A. M. Hagerstrom, T. E. Murphy, R. Roy, Cluster synchronization and isolated desynchronization in complex networks with symmetries. *Nat. Commun.* **5**, 4079 (2014).
4. D. S. Bassett, O. Sporns, Network neuroscience. *Nat. Neurosci.* **20**, 353–364 (2017).
5. J. M. Shine, P. G. Bissett, P. T. Bell, O. Koyejo, J. H. Balsters, K. J. Gorgolewski, C. A. Moodie, R. A. Poldrack, The dynamics of functional brain networks: Integrated network states during cognitive task performance. *Neuron* **92**, 544–554 (2016).
6. G. Deco, G. Tononi, M. Boly, M. L. Kringelbach, Rethinking segregation and integration: Contributions of whole-brain modelling. *Nat. Rev. Neurosci.* **16**, 430–439 (2015).
7. M. J. Panaggio, D. M. Abrams, Chimera states: Coexistence of coherence and incoherence in networks of coupled oscillators. *Nonlinearity* **28**, R67–R87 (2015).
8. O. E. Omel'chenko, Y. L. Maistrenko, P. A. Tass, Chimera states: The natural link between coherence and incoherence. *Phys. Rev. Lett.* **100**, 044105 (2008).
9. Y. Kuramoto, D. Battogtokh, Coexistence of coherence and incoherence in nonlocally coupled phase oscillators. *Nonlinear Phenom. Complex Syst.* **5**, 380–385 (2002).
10. D. M. Abrams, S. H. Strogatz, Chimera states for coupled oscillators. *Phys. Rev. Lett.* **93**, 174102 (2004).
11. M. R. Tinsley, S. Nkomo, K. Showalter, Chimera and phase-cluster states in populations of coupled chemical oscillators. *Nat. Phys.* **8**, 662–665 (2012).
12. A. M. Hagerstrom, T. E. Murphy, R. Roy, P. Hövel, I. Omelchenko, E. Schöll, Experimental observation of chimeras in coupled-map lattices. *Nat. Phys.* **8**, 658–661 (2012).
13. J. D. Hart, K. Bansal, T. E. Murphy, R. Roy, Experimental observation of chimera and cluster states in a minimal globally coupled network. *Chaos* **26**, 094801 (2016).
14. C. R. Laing, Chimeras in networks with purely local coupling. *Phys. Rev. E* **92**, 050904 (2015).
15. G. C. Sethia, A. Sen, Chimera states: The existence criteria revisited. *Phys. Rev. Lett.* **112**, 144101 (2014).
16. S. A. M. Loos, J. C. Claussen, E. Schöll, A. Zakharova, Chimera patterns under the impact of noise. *Phys. Rev. E* **93**, 012209 (2016).
17. C. R. Laing, Chimera states in heterogeneous networks. *Chaos* **19**, 013113 (2009).
18. I. Omelchenko, O. E. Omel'chenko, P. Hövel, E. Schöll, When nonlocal coupling between oscillators becomes stronger: Patched synchrony or multichimera states. *Phys. Rev. Lett.* **110**, 224101 (2013).
19. J. Xie, E. Knobloch, H.-C. Kao, Multicluster and traveling chimera states in nonlocal phase-coupled oscillators. *Phys. Rev. E* **90**, 022919 (2014).
20. A. Zakharova, M. Kapeller, E. Schöll, Chimera death: Symmetry breaking in dynamical networks. *Phys. Rev. Lett.* **112**, 154101 (2014).
21. V. Menon, Large-scale brain networks and psychopathology: A unifying triple network model. *Trends Cogn. Sci.* **15**, 483–506 (2011).
22. R. G. Andrzejak, C. Rummel, F. Mormann, K. Schindler, All together now: Analogies between chimera state collapses and epileptic seizures. *Sci. Rep.* **6**, 23000 (2016).
23. B. K. Bera, D. Ghosh, M. Lakshmanan, Chimera states in bursting neurons. *Phys. Rev. E* **93**, 012205 (2016).
24. J. Hizanidis, N. E. Kouvaris, G. Zamora-López, A. Díaz-Guilera, C. G. Antonopoulos, Chimera-like states in modular neural networks. *Sci. Rep.* **6**, 19845 (2016).
25. M. S. Santos, J. D. Szezech, F. S. Borges, K. C. Iarosz, I. L. Caldas, A. M. Batista, R. L. Viana, J. Kurths, Chimera-like states in a neuronal network model of the cat brain. *Chaos, Solitons Fractals* **101**, 86–91 (2017).
26. K. Bansal, J. D. Medaglia, D. S. Bassett, J. M. Vettel, S. F. Muldoon, Data-driven brain network models differentiate variability across language tasks. *PLOS Comput. Biol.* **14**, e1006487 (2018).
27. S. F. Muldoon, F. Pasqualetti, S. Gu, M. Cieslak, S. T. Grafton, J. M. Vettel, D. S. Bassett, Stimulation-based control of dynamic brain networks. *PLOS Comput. Biol.* **12**, e1005076 (2016).
28. J. D. Power, A. L. Cohen, S. M. Nelson, G. S. Wig, K. A. Barnes, J. A. Church, A. C. Vogel, T. O. Laumann, F. M. Miezin, B. L. Schlaggar, S. E. Petersen, Functional network organization of the human brain. *Neuron* **72**, 665–678 (2011).
29. H. R. Wilson, J. D. Cowan, Excitatory and inhibitory interactions in localized populations of model neurons. *Biophys. J.* **12**, 1–24 (1972).
30. K. Bansal, J. Nakuci, S. F. Muldoon, Personalized brain network models for assessing structure–function relationships. *Curr. Opin. Neurobiol.* **52**, 42–47 (2018).
31. L. L. Gollo, J. A. Roberts, L. Cocchi, Mapping how local perturbations influence systems-level brain dynamics. *Neuroimage* **160**, 97–112 (2017).
32. A. Spiegler, E. C. A. Hansen, C. Bernard, A. R. McIntosh, V. K. Jirsa, *eNeuro*, in press, doi:10.1523/ENEURO.0068-16.2016.
33. Y. Kuramoto, Self-entrainment of a population of coupled non-linear oscillators, in *International Symposium on Mathematical Problems in Theoretical Physics*, H. Araki, Ed. (Springer, 1975), vol. 39, pp. 420–422.
34. M. Shanahan, Metastable chimera states in community-structured oscillator networks. *Chaos* **20**, 013108 (2010).
35. M. P. van den Heuvel, O. Sporns, Rich-club organization of the human connectome. *J. Neurosci.* **31**, 15775–15786 (2011).
36. D. L. Sheinberg, N. K. Logothetis, Noticing familiar objects in real world scenes: The role of temporal cortical neurons in natural vision. *J. Neurosci.* **21**, 1340–1350 (2001).
37. C. Gratton, T. O. Laumann, A. N. Nielsen, D. J. Greene, E. M. Gordon, A. W. Gilmore, S. M. Nelson, R. S. Coalson, A. Z. Snyder, B. L. Schlaggar, N. U. F. Dosenbach, S. E. Petersen, Functional brain networks are dominated by stable group and individual factors, not cognitive or daily variation. *Neuron* **98**, 439–452.e5 (2018).
38. J. Scholz, M. C. Klein, T. E. J. Behrens, H. Johansen-Berg, Training induces changes in white-matter architecture. *Nat. Neurosci.* **12**, 1370–1371 (2009).
39. D. S. Margulies, J. L. Vincent, C. Kelly, G. Lohmann, L. Q. Uddin, B. B. Biswal, A. Villringer, F. X. Castellanos, M. P. Milham, M. Petrides, Precuneus shares intrinsic functional architecture in humans and monkeys. *Proc. Natl. Acad. Sci. U.S.A.* **106**, 20069–20074 (2009).
40. C. F. Stevens, An evolutionary scaling law for the primate visual system and its basis in cortical function. *Nature* **411**, 193–195 (2001).
41. A. P. Alivisatos, M. Chun, G. M. Church, R. J. Greenspan, M. L. Roukes, R. Yuste, The brain activity map project and the challenge of functional connectomics. *Neuron* **74**, 970–974 (2012).
42. S. M. Smith, P. T. Fox, K. L. Miller, D. C. Glahn, P. M. Fox, C. E. Mackay, N. Filippini, K. E. Watkins, R. Toro, A. R. Laird, C. F. Beckmann, Correspondence of the brain's functional architecture during activation and rest. *Proc. Natl. Acad. Sci. U.S.A.* **106**, 13040–13045 (2009).
43. R. Liégeois, E. Ziegler, C. Phillips, P. Geurts, F. Gómez, M. A. Bahri, B. T. Yeo, A. Soddu, A. Vanhaudenhuyse, S. Laureys, R. Sepulchre, Cerebral functional connectivity periodically (de)synchronizes with anatomical constraints. *Brain Struct. Funct.* **221**, 2985–2997 (2016).
44. J. M. Shine, M. J. Aburn, M. Breakspear, R. A. Poldrack, The modulation of neural gain facilitates a transition between functional segregation and integration in the brain. *eLife* **7**, e31130 (2018).
45. N. A. Crossley, A. Mechelli, J. Scott, F. Carletti, P. T. Fox, P. Mcguire, E. T. Bullmore, The hubs of the human connectome are generally implicated in the anatomy of brain disorders. *Brain* **137**, 2382–2395 (2014).
46. L. Cocchi, A. Zalesky, A. Fornito, J. B. Mattingley, Dynamic cooperation and competition between brain systems during cognitive control. *Trends Cogn. Sci.* **17**, 493–501 (2013).
47. M. A. Powell, J. O. Garcia, F.-C. Yeh, J. M. Vettel, T. Verstynen, Local connectome phenotypes predict social, health, and cognitive factors. *Netw. Neurosci.* **2**, 86–105 (2018).
48. D. Vatansever, D. K. Menon, A. E. Manktelow, B. J. Sahakian, E. A. Stamatakis, Default mode network connectivity during task execution. *Neuroimage* **122**, 96–104 (2015).
49. D. Vatansever, D. K. Menon, E. A. Stamatakis, Default mode contributions to automated information processing. *Proc. Natl. Acad. Sci. U.S.A.* **114**, 12821–12826 (2017).
50. T. D. Verstynen, The organization and dynamics of corticostriatal pathways link the medial orbitofrontal cortex to future behavioral responses. *J. Neurophysiol.* **112**, 2457–2469 (2014).
51. F. C. Yeh, W. Y. I. Tseng, NTU-90: A high angular resolution brain atlas constructed by q-space diffeomorphic reconstruction. *Neuroimage* **58**, 91–99 (2011).
52. F. C. Yeh, T. D. Verstynen, Y. Wang, J. C. Fernández-Miranda, W. Y. I. Tseng, Deterministic diffusion fiber tracking improved by quantitative anisotropy. *PLOS ONE* **8**, e80713 (2013).
53. G. S. Jeub, Lucas, M. Bazzi, I. S. Jutla, P. J. M. Mucha, A generalized Louvain method for community detection implemented in MATLAB; http://netwiki.amath.unc.edu/GenLouvain).
54. D. S. Bassett, M. A. Porter, N. F. Wymbs, S. T. Grafton, J. M. Carlson, P. J. Mucha, Robust detection of dynamic community structure in networks. *Chaos* **23**, 013142 (2013).
55. M. Rubinov, O. Sporns, Complex network measures of brain connectivity: Uses and interpretations. *Neuroimage* **52**, 1059–1069 (2010).
56. M. Xia, J. Wang, Y. He, BrainNet Viewer: A network visualization tool for human brain connectomics. *PLOS ONE* **8**, e68910 (2013).

Acknowledgments: We acknowledge G. Lieberman for the preprocessing of the brain anatomical connectivity data and R. Roy and J. D. Hart for a useful discussion on chimera states. **Funding:** This work is supported by the Army Research Laboratory through contract nos. W911NF-10-2-0022 and W911NF-17-2-0158 from the U.S. Army Research Office. The views and conclusions contained in this document are those of the authors and should not be interpreted as representing the official policies, either expressed or implied, of the Army Research Laboratory or the U.S. government. The U.S. government is authorized to reproduce and distribute reprints for government purposes notwithstanding any copyright notation herein. **Author contributions:** K.B. conceived the idea. K.B., J.M.V., and S.F.M. designed the

research. T.V. and J.M.V. collected the data. S.F.M. developed the BNM. K.B. implemented the model and led the analysis. All authors contributed analysis ideas and wrote the paper.
Competing interests: The authors declare that they have no competing interests.
Data and materials availability: All data needed to evaluate the conclusions in the paper are present in the paper and/or the Supplementary Materials. Additional data related to this paper may be requested from the authors. Data are also publicly available on Zenodo (doi:10.5281/zenodo.2590868; https://zenodo.org/record/2590869).

Submitted 20 July 2018
Accepted 13 February 2019
Published 3 April 2019
10.1126/sciadv.aau8535

Citation: K. Bansal, J. O. Garcia, S. H. Tompson, T. Verstynen, J. M. Vettel, S. F. Muldoon, Cognitive chimera states in human brain networks. *Sci. Adv.* **5**, eaau8535 (2019).

Cognitive chimera states in human brain networks

Kanika Bansal, Javier O. Garcia, Steven H. Tompson, Timothy Verstynen, Jean M. Vettel and Sarah F. Muldoon

Sci Adv **5** (4), eaau8535.
DOI: 10.1126/sciadv.aau8535